EARTH SURFACE PROCESSES AND LANDFORMS
Earth Surf. Process. Landforms (2017)

Published online in Wiley Online Library
(wileyonlinelibrary.com) DOI: 10.1002/esp.4205

Spatial and temporal replicability of meteoric and *in situ* ^{10}Be concentrations in fluvial sediment

Veronica Sosa Gonzalez,[1] Amanda H. Schmidt,[2*] Paul R. Bierman[1] and Dylan H. Rood[3,4,5]
[1] Geology Department and Rubenstein School of the Environment and Natural Resources, University of Vermont, Burlington, VT USA
[2] Geology Department, Oberlin College, Oberlin, OH USA
[3] Department of Earth Science and Engineering, Imperial College London, London, UK
[4] Accelerator Mass Spectrometry Laboratory, Scottish Universities Environmental Research Centre, East Kilbride, UK
[5] Earth Research Institute, University of California, Santa Barbara, CA USA

Received 8 March 2017; Revised 6 July 2017; Accepted 17 July 2017

*Correspondence to: Amanda H. Schmidt, Geology Department, Oberlin College, Oberlin, OH 44074, USA. E-mail: amanda.schmidt@oberlin.edu

ESPL
Earth Surface Processes and Landforms

ABSTRACT: Cosmogenic isotopes, short-lived radionuclides, elemental concentrations and thermochronometric indicators are measured in river sand to quantify erosion rates and trace sediment sources, and/or infer erosional processes. Interpretations of detrital sediment analyses are often based on the rarely tested assumption of time-invariant tracer concentration. A better understanding of when and where this assumption breaks down and what sampling strategies minimize temporal and small-scale spatial variance will improve science done using detrital river sediment.

Here, we present new and previously published spatial and temporal replicates measured for *in situ* and meteoric ^{10}Be (^{10}Be$_i$ and ^{10}Be$_m$, respectively). Our new data include 113 replicate pairs, taken from agricultural and/or tectonically active watersheds in China months to millennia apart and spatial replicates taken up to 2 km apart on the same day. The mean percentage difference is 10% (−122% to 150%) for both systems considered together; the mode is close to 0% for both systems; and 36% of pairs of samples replicate within our analytical accuracy at 2σ. We find that ^{10}Be$_i$ replicates better than ^{10}Be$_m$ ($p < 0.01$). ^{10}Be$_i$ replicability is worse in steeper basins, suggesting that stochastic processes (i.e. landslides) affect reproducibility. ^{10}Be$_m$ replicability is worse in larger basins, suggesting non-conservative behavior of ^{10}Be$_m$ as sediment moves downstream.

Our results are consistent with the few previously published replicate studies. Considering all replicate data in a wide range of landscapes, in areas with deep erosional processes, replicability is poor; in other areas, replicability is good. This suggests that, in steep, tectonically active, and/or agricultural landscapes, individual detrital sediment measurements do not represent upstream rates as well as larger populations of samples. To ensure that measurements are representative of the upstream watershed, our data suggest that samples be amalgamated either over time or from several places close by in the same channel. Copyright © 2017 John Wiley & Sons, Ltd.

KEYWORDS: temporal replicates; spatial replicates; cosmogenic; variability; detrital sediment

Introduction

Commonly employed geological techniques, including detrital thermochronology (Bernet and Spiegel, 2004), chemical fingerprinting and tracing of sediment sources (Clapp *et al.*, 2002; Reusser and Bierman, 2010; Owens *et al.*, 2016), and cosmogenic radionuclide estimation of erosion rates (Brown *et al.*, 1995; Bierman and Steig, 1996; Granger *et al.*, 1996), assume that detrital river sediment represents an integrated sample of material shed by the upstream landscape. Accurate interpretation relies on the assumptions that the sediment sampled in a river is homogenized, that sampled sediment represents an integration of the entire upstream basin, and that the concentration of the analyte of interest is steady over the time period over which the analysis integrates.

These assumptions are most likely to break down in landscapes subjected to intensive human land use and those affected by stochastic erosional processes, such as landslides due to tectonic activity, steep slopes or large rain events (Niemi *et al.*, 2005). Conversely, some research relies on the breakdown of these assumptions and uses temporal and spatial variability in sediment to discern changing landscape processes (Clapp *et al.*, 2002; Schaller et al., 2002; Ruhl and Hodges, 2005; Vermeesch, 2007; McPhillips and Brandon, 2010; Reusser and Bierman, 2010; Lupker *et al.*, 2012; McPhillips *et al.*, 2014; West *et al.*, 2014; Herman *et al.*, 2015; Schaller et al., 2016; Zhang *et al.*, 2017). However, when the goal is to determine basin average values, studies assume that sediment is well mixed. In this paper, we test the assumption that detrital fluvial sediment is well mixed for cosmogenic ^{10}Be and use the results to propose sampling strategies relevant to all techniques using detrital sediment samples to represent upstream catchment processes.

Although testing reproducibility is not as eye catching as presenting new conclusions about the way the world works, formal testing of replicability in research results is increasingly

recognized as fundamental to the process of doing science. The American Association for the Advancement of Science (McNutt, 2014; Buck, 2015; Goodman *et al.*, 2016; Rosenblatt, 2016), the American Geophysical Union (Goldstein *et al.*, 2014; Hanson and Hilst, 2014), Sigma Xi (Wainer, 2012), the Nature Publishing Group (Editorial Staff, 2016a, 2016b, 2016c, 2017), the National Science Foundation (NSF, 2014, 2016) and the National Institutes for Health (NIH, 2016a, 2016b) have all recently opened discussions calling for increased focus on reproducibility. In particular, an editorial in *Nature* argues, 'To make replication studies more useful, researchers must make more of them, funders must encourage them and journals must publish them' (Editorial Staff, 2016a).

With many geological techniques relying increasingly on detrital samples as representative of upstream catchment areas and using the resulting data to infer tectonic and climatic processes, investigating reproducibility is fundamental to Earth science. One widely used geological technique relies on detrital samples for calculating erosion rates from basin-average *in situ* ^{10}Be (Brown *et al.*, 1995; Bierman and Steig, 1996; Granger *et al.*, 1996), a cosmogenic radionuclide produced in rock and soil (Lal, 1991). A 2016 compilation reports over 70 published datasets with nearly 1500 estimates of basin-average erosion rates (Harel *et al.*, 2016); however, because that work was based on two prior compilations, published in 2011 and 2013 (Portenga and Bierman, 2011; Willenbring *et al.*, 2013), many more recent studies are not included and thus the number of relevant studies and measurements is now far higher.

The temporal variability of cosmogenic ^{10}Be concentration in river sediment has been infrequently studied, and most studies have analyzed only a few samples. Temporal variation of *in situ* ^{10}Be (^{10}Be$_i$) over millennial timescales has been assessed by comparing isotopic activity of river terraces and active channel sediments in France, the Netherlands and Madagascar (Schaller et al., 2002; Cox *et al.*, 2009; Schaller et al., 2016). When observed, variations in isotope concentration are attributed to stochastic processes such as deep-seated landslides (Lupker *et al.*, 2012; West *et al.*, 2014) and debris flows (Kober *et al.*, 2012), which have a proportionally greater effect on small watersheds (Reusser and Bierman, 2010), changing sediment sourcing following a large storm (Foster and Anderson, 2016) or millennial timescale climate change altering erosion rates (Schaller *et al.*, 2002, 2016). Replication of meteoric ^{10}Be (^{10}Be$_m$) has only been tested once: larger basins replicated within analytical error, but some smaller basins did not (Reusser and Bierman, 2010). Modeling suggests that widespread landsliding in a watershed can increase temporal variability in isotopic concentration of sampled sediment (Niemi *et al.*, 2005; Yanites *et al.*, 2009), especially in small ($<$100 km^2) watersheds dominated by deep ($>$5 m) landslides (Yanites *et al.*, 2009).

In this paper, we quantify the variability of both ^{10}Be$_i$ and ^{10}Be$_m$ concentrations in river sediment over different time and spatial scales. To achieve this goal, we did two things. First, we compiled previously published replicate samples, and second, we analyzed the replicability of a set of samples collected in China and measured for other purposes (Neilson, 2015; Sosa Gonzalez, 2016). The new replicate samples were collected in a highly disturbed field area where the assumptions underpinning ^{10}Be$_i$ and ^{10}Be$_m$ methods are least likely to be viable due to tectonic activity, monsoonal rainfall, steep hillslopes and extensive human modification of the landscape. We consider 'disturbed' landscapes to be places where events such as earthquakes, agricultural land conversion and large storms could alter erosion processes and sediment sourcing substantially over time. In contrast, less disturbed landscapes have fewer events that alter the intensity and distribution of surface processes over time.

Because many landscapes in China have been disturbed by natural tectonic and climatic driven surface processes as well as human impacts on the landscape, it is a challenging place to apply the ^{10}Be method and so provides, in some ways, a 'worst case' test of replicability; however, China is not the only highly disturbed landscape in which cosmogenic nuclides have been measured. Many regions where ^{10}Be has been used for geomorphic analysis are tectonically active (Lupker *et al.*, 2012; West *et al.*, 2014), steep (Portenga *et al.*, 2015), subject to extreme rainfall events (Foster and Anderson, 2016) and/or have experienced widespread land use change (Hewawasam *et al.*, 2003; Reusser and Bierman, 2010; Schmidt *et al.*, 2016). By performing spatial and temporal replicate analyses in a setting where many factors are likely to increase the temporal and spatial heterogeneity of analyte concentration in sediment, our results illustrate the limitations of detrital sediment studies and inform sampling strategies not only for cosmogenic nuclides but also for all geochemical detrital sediment analyses.

Background

Using ^{10}Be to understand erosion

In situ-produced ^{10}Be (^{10}Be$_i$) is the most widely used cosmogenic isotope (Portenga and Bierman, 2011) because it accumulates in a common mineral (quartz) and is easily measured; furthermore, there is only one primary production pathway in quartz (Lal, 1991). It has been used since the 1990s to study erosion and sediment transport (Brown *et al.*, 1995; Bierman and Steig, 1996; Granger *et al.*, 1996). Most ^{10}Be$_i$ forms in the crystal lattice as the result of spallation reactions between secondary cosmic rays (primarily neutrons) and oxygen nuclei. This reaction occurs primarily near Earth's surface and is highly attenuated at depths greater than ~2 m (Lal, 1991). Thus ^{10}Be$_i$ is a good indicator of the near-surface residence time of rock and regolith, and denudation rates at both the outcrop and basin scale; ^{10}Be$_i$ concentration is inversely proportional to erosion rate.

Meteoric ^{10}Be (^{10}Be$_m$) forms in the atmosphere through cosmic-ray-induced spallation of nitrogen and oxygen nuclei (Lal and Peters, 1967). Once formed in the atmosphere, the isotope adheres to aerosols and is delivered to Earth's surface by either precipitation or dry deposition (Graly *et al.*, 2010). The delivery of ^{10}Be$_m$ is a function of latitude, precipitation rate and the movement of the isotope within the atmosphere (Willenbring and von Blanckenburg, 2010). Most ^{10}Be$_m$ resides in the upper few meters of soil and regolith (Graly *et al.*, 2010). Although ^{10}Be$_m$ has been used less than ^{10}Be$_i$ for geomorphology, it is increasing in popularity (Willenbring and von Blanckenburg, 2010). ^{10}Be$_m$ has been used to trace sediment at the watershed scale (e.g. Reusser and Bierman, 2010) and to estimate soil loss rates (Brown *et al.*, 1988). More recent work uses ^{10}Be$_m$ in conjunction with stable ^{9}Be to assess catchment average denudation, weathering and erosion rates (von Blanckenburg et al., 2012). The concentration of ^{10}Be$_m$ in sediment reflects the near surface residence time of the sample (Wittmann *et al.*, 2015).

Factors that could affect replication

Prior studies suggest four factors that may influence whether replicate detrital sediment samples have analyte concentrations within uncertainty of one another for a particular basin: upstream basin area, mean basin slope, mean annual

precipitation and the intensity of land disturbance by human activities in the upstream watershed (Matmon *et al.*, 2003; Niemi *et al.*, 2005; Binnie *et al.*, 2006; Savi *et al.*, 2014). Increased upstream areas are associated with better mixing of detrital sediments (e.g. Matmon *et al.*, 2003), suggesting that replicate samples will be more similar in larger basins. Increased basin steepness, up to the maximum steepness slopes, can hold without failing (Montgomery and Brandon, 2002; Binnie *et al.*, 2007) may be associated with increases in high-magnitude, low-frequency events (e.g. debris flows and landslides). Such mass movements episodically deliver deeply sourced sediment with low concentrations of cosmogenic isotopes. Similarly, increased precipitation, particularly concentrated in the monsoon season (Yang *et al.*, 2010), could also increase the likelihood of debris flows and landslides, episodically altering the isotopic concentration of channel sediment (Niemi *et al.*, 2005; Binnie *et al.*, 2006; Savi *et al.*, 2014). Upstream agricultural land use increases modern sediment yield relative to long-term rates of sediment generation (Hewawasam *et al.*, 2003; Schmidt *et al.*, 2016) through increased linear erosional features or widespread sheetwash (Von Blanckenburg *et al.*, 2004). Such rapid sediment transfer mechanisms could increase sediment yield from one part of the basin only during certain times of the year, thus seasonally affecting the isotopic concentration of in channel sediment.

Methods

Existing data compilation

We surveyed the literature in order to find studies that included either spatial (two sites <2 km apart taken on the same day) or temporal replicate collections of fluvial sand in order to have a broad global dataset for analysis. We identified 87 pairs (n = 84 $^{10}Be_i$, n = 3 $^{10}Be_m$) of replicate collections from 17 studies completed in China, Cameroon, Greenland, Madagascar, Panama, USA, Europe, New Zealand and the Himalayas (Table I). We did not recalculate any data from the papers for changed mass spectrometry standard values (Nishiizumi *et al.*, 2007) because the important comparison is percent difference in isotopic concentration (or erosion rate) between two time periods (or places) rather than derived concentrations (or erosion rates).

New Chinese data

At 33 sites in China, we collected sand-size (250–850 μm) sediment samples from active river channels and deposits from the most recent flood (hereafter 'overbank'; unvegetated areas immediately adjacent to the channel) to analyze for both $^{10}Be_i$ and $^{10}Be_m$ (Figure 1A). Details of sampling site geological context and original data are reported in Neilson (2015) and Sosa Gonzalez (2016). Alluvial terraces alongside rivers were present at some sites. Agriculture on river banks and dredging of river channels for gravel were common. When possible, we collected samples upstream of immediately identifiable dredging operations, although these sites were likely downstream of other dredging operations. With the exception of CH-149, CH-150 and CH-161 to CH-172, which were collected from a steep bedrock gorge, most samples were collected from alluvial rivers in primarily agricultural and forested landscapes. Agricultural land use varies from <1% to 50% in the sampled watersheds (Chen *et al.*, 2015).

Basin boundaries, upstream area and mean basin slope were derived from GDEM topography data (NASA LP-DAAC, 2012).

Table I. Details on the prior studies compiled for this analysis. All are temporal replicates. All compiled data are in Supporting Information Tables DR6 and DR7

Reference	Isotope	Number of replicates	Location	Range of erosion rates	Disturbance intensity
Cox *et al.* (2009)	$^{10}Be_i$	2	Madagascar	~0.012 mm yr^{-1}	High in some areas (lavakas)
Foster and Anderson (2016)	$^{10}Be_i$	13	Colorado Front Range	0.02–0.05 mm yr^{-1}	Low, but replicates collected after a large flood
Godard *et al.* (2010)	$^{10}Be_i$	2	Sichuan, China	0.5–1 mm yr^{-1}	High – tectonically active and agricultural
Kober *et al.* (2012)	$^{10}Be_i$	9	Swiss Alps	1–2 mm yr^{-1}	High – replicates taken after debris flows
Lupker *et al.* (2012)	$^{10}Be_i$	8	Nepal	Mean = 1.3 mm yr^{-1}	Moderate – taken before recent earthquakes, but tectonically active
Matmon *et al.* (2003)	$^{10}Be_i$	1	Great Smoky Mountains	0.03 mm yr^{-1}	Minimal
Nelson *et al.* (2014)	$^{10}Be_i$	9	Greenland	N/A[a]	High[a]
Palumbo *et al.* (2011)	$^{10}Be_i$	1	Tibet	0.3 mm yr^{-1}	Minimal
Portenga *et al.* (2015)	$^{10}Be_i$	1	Bhutan	0.4 mm yr^{-1}	Moderate – tectonically active
Regard *et al.* (2016)	$^{10}Be_i$	3	Cameroon	0.01–0.1 mm yr^{-1}	Moderate – agricultural
Reusser and Bierman (2010)	$^{10}Be_m$	3	New Zealand	Not reported	High in headwaters
Reusser *et al.* (2017)	$^{10}Be_i$	1	Eastern USA	0.009 mm yr^{-1}	Minimal
Schaller *et al.* (2002)	$^{10}Be_i$-derived erosion rates	11	France, Netherlands	0.03–0.08 mm yr^{-1}	Minimal
Schaller *et al.* (2016)	$^{10}Be_i$-derived erosion rates	11	Europe	0.01–0.08 mm yr^{-1}	Minimal
Sosa Gonzalez *et al.* (2016)	$^{10}Be_i$	2	Panama	Mean = 0.14 mm yr^{-1}	Minimal
Vance *et al.* (2003)	$^{10}Be_i$	1	Nepal	0.9 mm yr^{-1}	Moderate – taken before recent earthquakes, but tectonically active
West *et al.* (2014)	$^{10}Be_i$	9	Sichuan, China	Not reported	High – replicates taken after 2008 Wenchuan earthquake

[a]These data were used for sediment source analyses and are exceptionally low concentration (10^3 atoms g^{-1}). They are proglacial sediments and cannot be used for erosion rates. Disturbance in this case is considered to be frequent large outburst floods.

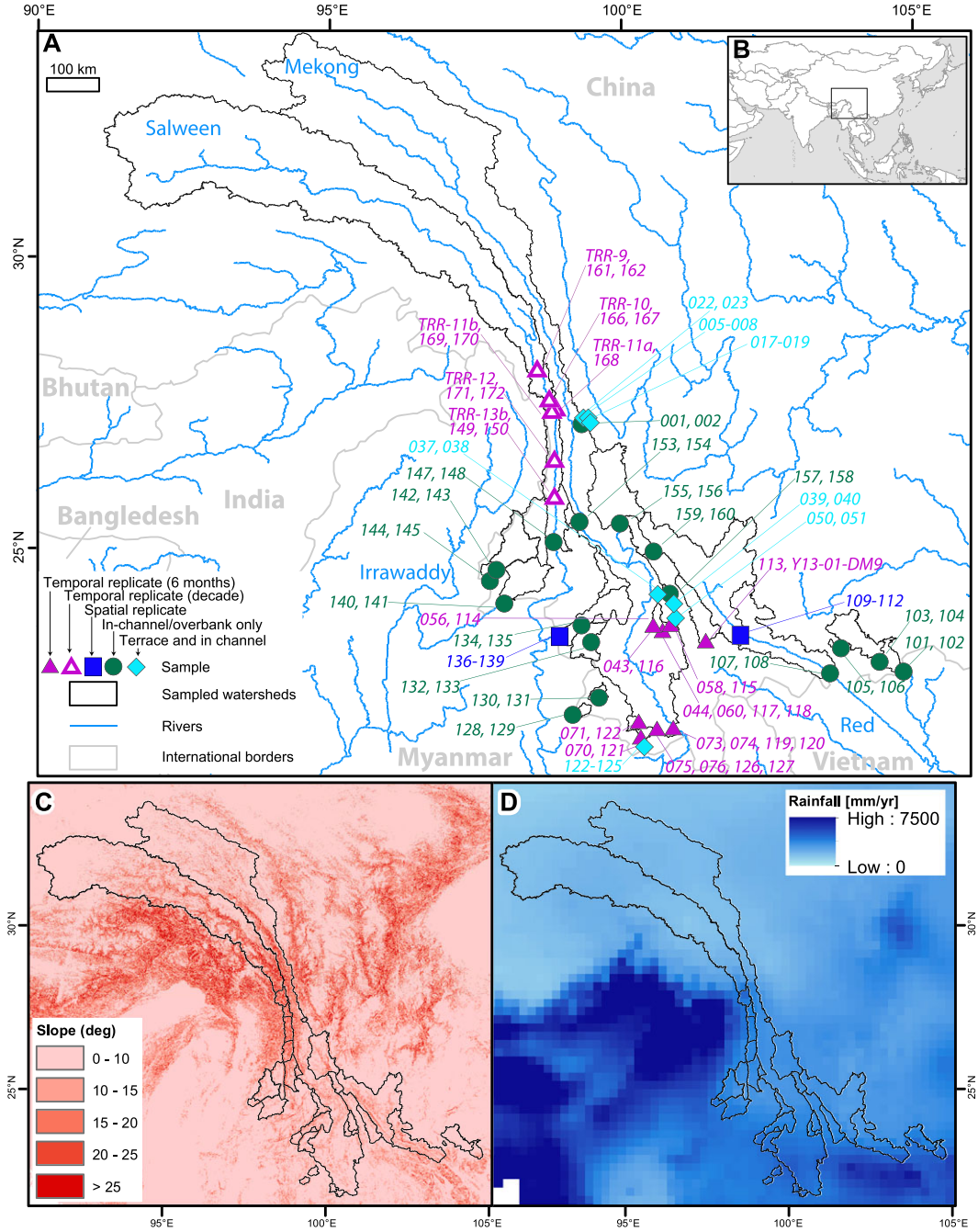

Figure 1. Overview map of the study site. (A) Sample points and the upstream area they sample are shown, with nearby countries and rivers for reference. Samples with 0xx numbers and Y13-01-DM09 were sampled in 2013, samples with 1xx numbers were sampled in 2014, and samples with TRR numbers were sampled in 2005. (B) Context of the study area in Asia with box showing location of panels A, C and D. (C) Distribution of slopes throughout the study area. Slope data are derived from GDEM data (NASA LP-DAAC, 2012). (D) Distribution of rainfall in the study area. Rainfall data are from APHRODITE (Yatagai *et al.*, 2012). For geology, topography and land use information about the sites, see Supporting Information figure DR1. [Colour figure can be viewed at wileyonlinelibrary.com]

Mean basin rainfall was derived from APHRODITE data (Yatagai *et al.*, 2012), which has lower spatial resolution than other available datasets but better temporal and spatial accuracy (Andermann *et al.*, 2011). Land use was derived from the Global Land Cover project (Chen *et al.*, 2015). The uncertainty inherent in these datasets is not known.

Eleven sites were sampled in May - June 2013 just as the monsoon was beginning (series CH-0XX), and resampled in January 2014 during the dry season (series CH-1XX). An additional replicate sample was collected by D. McPhillips (Y-13-01-DM) in May 2013 approximately 2 km downstream from our CH-113 sample; we analyzed both samples (Table II). In this case, where the sample is both a temporal and spatial replicate, we consider it as just a temporal replicate. Seven sites were sampled in October 2005 (series TRR-xx), and resampled in January 2014 during the dry season (CH-149, CH-153, CH-161, CH-167, CH-168, CH-169, CH-171). When these samples were first analyzed, the $^{10}Be_i$ concentration was so different from the 2005 TRR samples (30–95% higher) that we wanted to be certain that the difference was not due to processing the samples a decade apart in two different labs and analyzing them on two different accelerators. Therefore, we went back to the original TRR samples and ran them as lab replicates. The data we report for the TRR samples are the error-weighted average of Henck *et al.'s* (2010) TRR data (renormalized to the same normalization used for the CH samples) and the new lab replicate data. The TRR $^{10}Be_m$ data reported here are newly analyzed for this project from original

Table II. Number of samples included per category for new China data

Analysis	Isotope analyzed	Number of samples included	Sample year
Temporal replicates – 6 months	$^{10}Be_i$	24 (12 pairs)	2013/2014
	$^{10}Be_m$	20 (10 pairs)	2013/2014
Temporal replicates – in-channel/overbank	$^{10}Be_i$	64 (32 pairs)	2013/2014
	$^{10}Be_m$	58 (29 pairs)	2013/2014
Spatial replicates – samples taken <2 km apart from one another on the same day	$^{10}Be_i$	8 (4 pairs, 2 sites)	2014
	$^{10}Be_m$	8 (4 pairs, 2 sites)	2014
Temporal replicates – millennial, terrace sand	$^{10}Be_i$	18 (9 pairs)	2013/2014
Temporal replicates – decadal	$^{10}Be_i$	10 (5 pairs)	2005/2014
	$^{10}Be_m$	12 (6 pairs)	2005/2014

TRR sand. We also include three laboratory processing replicates for $^{10}Be_i$ (CH-002(A), CH-137(A) and CH-148(A)) (Supporting Information Table DR1). To test for seasonal bias of sediment sourcing, we sampled sediment from the active channel during dry season base flow and adjacent overbank sediment deposited during the previous monsoon flood season. When alluvial terraces alongside the river contained charcoal, we sampled charcoal and sand-size material deposited in the same stratum as a long-term resample of active river sediment (see Supporting Information Figure DR2 for stratigraphic columns of terraces we sampled). We radiocarbon dated the charcoal at the W. M. Keck Carbon Cycle Accelerator Mass Spectrometry Laboratory, CA, USA (Santos *et al.*, 2007; Supporting Information Table DR2).

Quartz from the samples was isolated and purified using a modification of the method of Kohl and Nishiizumi (1992). $^{10}Be_i$ was extracted from quartz following the method of Corbett *et al.* (2016). Each batch contained one process blank and one CRONUS N standard (Jull *et al.*, 2015) (see Supporting Information Table DR3a for CRONUS N results). After the quartz was dissolved in hydrofluoric acid, aliquots were removed and analyzed by inductively coupled plasma–optical emission spectroscopy (ICP-OES) to measure Be and Al concentration (Portenga *et al.*, 2015; Corbett *et al.*, 2016); 24 samples had Be recovery > 100% (range: 106.2–198.1%) (based on the Be carrier added), indicating the presence of native Be in those samples.

We milled bulk samples (sieved to isolate the sand fraction (250–850 μm)) and analyzed them for $^{10}Be_m$. A small portion (~0.5 g) of pulverized material was used for isotopic extraction. We used a modification of the method of Stone (1998) to extract $^{10}Be_m$. Each batch contained one STA1(KFA) internal standard (see Supporting Information Table DR3b for STA1(KFA) data).

Isotopic ratios for the CH samples and TRR $^{10}Be_m$ analyses were measured using accelerator mass spectrometry (AMS) at the Scottish Universities Environmental Research Centre in East Kilbride, Scotland (Xu *et al.*, 2015) and normalized to the NIST standard with an assumed $^{10}Be/^{9}Be$ ratio of 2.79×10^{-11} (Nishiizumi *et al.*, 2007) (Supporting Information Table DR1); TRR lab replicates were analyzed at Lawrence Livermore National Labs. Secondary standards measured over all four of the AMS campaigns indicate 2–3% total precision and accuracy for the KN62 AMS standard; this standard material is the closest ratio to the measurements of the CRONUS N standard material and within the quoted analytical uncertainty of the CRONUS N measurements. Thus the AMS precision and accuracy in this ratio range are 2–3% (1σ) for all of the runs in which China samples were measured. Background correction was done using full process blanks, one of which was run with each batch of 10 samples. For the samples with native ^{9}Be, we used the total Be from ICP measurements to calculate ^{10}Be concentration, rather than the amount of Be added as carrier (cf. Portenga *et al.*, 2015). The final uncertainty of the blank-corrected ratio is the uncertainty of the isotopic measurement and the blank propagated in quadrature.

Statistical analysis

To quantify temporal variations in isotopic concentrations, we used the following equation:

$$\frac{N_1 - N_2}{\frac{N_1+N_2}{2}} \quad (1)$$

where N_1 is the original (or overbank for interannual replicates) sample and N_2 is the replicate (or in-channel for interannual replicates) sample. We express the result as a percentage.

The nine measurements of the CRONUS N standards replicated with a scatter of 6.4% (1σ). Thus we consider 13% as the two-sigma (2σ) precision due to accumulated errors in laboratory processing, cathode packing and sample measurement for $^{10}Be_i$ analyses (which exceeds average measurement precision for individual measurements and the scatter in the secondary AMS standards by about two times; Supporting Information Tables DR1 and DR3a). The five measurements of the STA1(KFA) standard replicate with a scatter of 3.50% (1σ). Thus we consider 7% as the 2σ precision due to accumulated errors in laboratory processing, cathode packing and sample measurement for $^{10}Be_m$ analyses (which also exceeds average measurement precision for individual measurements and the scatter in the secondary AMS standards by about two times; Supporting Information Tables DR1 and DR3b). Our definition of sample replication sets a conservative limit on what we identify as a significant difference in isotopic concentrations among replicates and enables us to quantify geological variation beyond analytical uncertainty.

To test for whether populations of samples are different, we use a Wilcoxon signed-rank test (a paired difference test). The null hypothesis for the test is that the two sets of samples are drawn from the same population and the alternate hypothesis is that the samples are from different populations; thus the *p*-value returned is the probability that the sample populations are the same. Smaller *p*-values mean that the two sets of data being compared are less likely to be from the same population. For this test, we compare isotopic concentrations rather than percent difference.

When testing whether replicability is different for $^{10}Be_i$ and $^{10}Be_m$, we use the Mann–Whitney U-test (an unpaired signed rank difference test). This nonparametric test does not require

that populations are the same size. In this case, we compare the absolute value of the replicability of pairs of samples because the goal is to quantify how different they are from each other rather than whether they are above or below 0. We then normalize the data to account for the different lab replicability of the two Be isotopic systems (2σ = 13% for $^{10}Be_i$ and 7% for $^{10}Be_m$). To do this, we divide the absolute value of each sample pair's replicability by the 2σ value (i.e., percent replicability divided by 13 for $^{10}Be_i$ and percent replicability divided by 7 for $^{10}Be_m$).

Results

New Chinese data

Considering our entire dataset of 113 pairs of Chinese samples, we cannot statistically distinguish ($p = 0.49$ for both $^{10}Be_m$ and $^{10}Be_i$) the difference in populations of samples taken at different times or slightly different places for any isotope or any type of resampling, but there is a large variability in the differences between the concentrations of individual replicate pairs (Figure 2, Table III and Supporting Information Table DR4). In cases where both $^{10}Be_m$ and $^{10}Be_i$ were measured in the same sample, the percentage difference for a given paired sample measurement of $^{10}Be_i$ is correlated to the percentage difference for that paired sample's concentration of $^{10}Be_m$ ($R = 0.430$, $p < 0.01$) (Figure 3).

We find that $^{10}Be_i$ replicates better than $^{10}Be_m$, with four times as many pairs of samples replicating within 2σ for $^{10}Be_i$ than for $^{10}Be_m$ ($p < 0.01$ for the Mann–Whitney U-test). Laboratory replicability of internal standards is better for $^{10}Be_m$ than $^{10}Be_i$ (twice the standard deviation of replicate analyses for STA1(KFA) [$^{10}Be_m$] [2σ] = 7% while twice the standard deviation of replicate analyses for STAN-N [$^{10}Be_i$] [2σ] = 13%). Thus the poorer replicability for $^{10}Be_m$ for field samples is not due to the different sample processing procedures.

Landscape scale factors exert at most weak control on replication. There is no correlation between upstream area and replication for $^{10}Be_i$, but there is a correlation for $^{10}Be_m$ such that increased basin area leads to worse replicability (Figures 4A, 4B). Steeper basins tend to have greater differences in $^{10}Be_i$ between replicate samples (Figure 4C) but mean basin slope does not affect $^{10}Be_m$ replication (Figure 4D). Increased mean annual precipitation correlates with better replicability of $^{10}Be_i$ (Figure 4E) but not $^{10}Be_m$ (Figure 4F). Finally, the fraction of the upstream basin that is agricultural correlates with replication for $^{10}Be_i$ but not $^{10}Be_m$ such that more agricultural basins replicate better (Figures 4G, 4H).

We find that mean annual precipitation, slope and upstream agricultural land use are all correlated (albeit not well) with replication of $^{10}Be_i$ in samples. However, all three parameters are significantly correlated with one another ($|R| \geq 0.69$, $p < 0.01$); the correlation between slope and both rainfall and agricultural land use are negative (Supporting Information Figure DR3). This correlation suggests that the weak correlations we find between replicability and both agricultural land use and rainfall (where increases in rainfall and agricultural land use result in better replicability) may be a function of slope rather than caused by agricultural land use and rainfall.

Compilation of previously published results

Combining our new analysis (n = 113 total pairs: 64 $^{10}Be_i$ pairs and 49 $^{10}Be_m$ pairs) with previously published resampling data (n = 87 pairs, Table I) allows us to consider more broadly how well detrital sediments represent average upstream isotopic concentrations across a range of landscapes from natural and slowly eroding to heavily disturbed and/or tectonically active locations. $^{10}Be_i$ resamples taken from locations with relatively gentle topography and without extreme rainfall events, even if they have relatively widespread agriculture, including northern Tibet (Palumbo *et al.*, 2011), the Great Smoky Mountains (Matmon *et al.*, 2003) and the Appalachian Mountains (Reusser *et al.*, 2017), all replicate within 2σ (assuming 2σ is 13% for $^{10}Be_i$ and 7% for $^{10}Be_m$, based on analysis of our internal standards because no such data are provided in other studies). The only samples from these types of landscapes that do not replicate well are from Europe and document erosion rate changes over thousands to millions of years – differences which the authors attribute to long-timescale climatic changes (Schaller *et al.*, 2002, 2016).

In contrast, replicability in steep environments seems to vary depending on prevalence of deep erosional processes and not just hillslope steepness. Prior work in some steep locations, including the Himalayas – Nepal (Vance *et al.*, 2003); Bhutan (Portenga *et al.*, 2015) – and Panama (Sosa Gonzalez *et al.*, 2016), has found that samples replicate well. Likewise, a study of samples taken before and after a large flood draining steep basins in the Colorado Front Range finds that only three out of 13 samples do not replicate within 2σ (Foster and Anderson, 2016).

However, in small basins (<210 km^2) with deep erosional features, such as lavakas in Madagascar (Cox *et al.*, 2009) and debris flows in the Swiss Alps (Kober *et al.*, 2012), $^{10}Be_i$ does not replicate well. In these cases, the erosional features disproportionately and episodically contribute deeply sourced sediment. The stochastic nature of these mass movement processes in small watersheds means that sediment sources could easily and rapidly change, creating sediment pulses that move through the system (Miller and Benda, 2000; Gran and Czuba, 2017). In this case, sampled sediment may be from a pulse of sediment rather than representative of the average isotopic concentration of sediment moving through the channel over time at the sampling point (Kober *et al.*, 2012). Likewise, in steep, tectonically active environments – Sichuan, China (Godard *et al.*, 2010; West *et al.*, 2014) – where replicate sampling was done in the first few years after the 2008 Wenchuan earthquake, replicability is generally poor; the authors attribute observed variability to earthquake-induced landslides and debris flows moving large amounts of deeply sourced sediment to the channel. In contrast, in the Himalayas, where landslides are widespread and frequent throughout the mountain range, variability in concentration is attributed to changing sediment sources from different elevations with different concentrations of ^{10}Be due to altitudinally varying production rates (Lupker *et al.*, 2012). In Greenland, poor sample replicability is attributed to changing sediment sources on an annual timescale (Nelson *et al.*, 2014).

When we add our 64 pairs of $^{10}Be_i$ resamples to 87 previously published pairs of $^{10}Be_i$ resamples, we find the reproducibility of our samples is within the range of previously reported replicates (Figure 5A). Furthermore, the population of all $^{10}Be_i$ replicates (n = 151) has a mode within 2σ (13%) of 0 (lower right inset, Figure 5A).

There are only three previously published replicates of $^{10}Be_m$ analyses (Reusser and Bierman, 2010). These three samples were taken from the Waipaoa River basin in New Zealand, an area of weak mudstones with widespread logging and subsequent deep and extensive landsliding. Two of their samples replicate well; one, from a small (~100 km^2) basin, does not. Thus all the meteoric replicates done so far are from

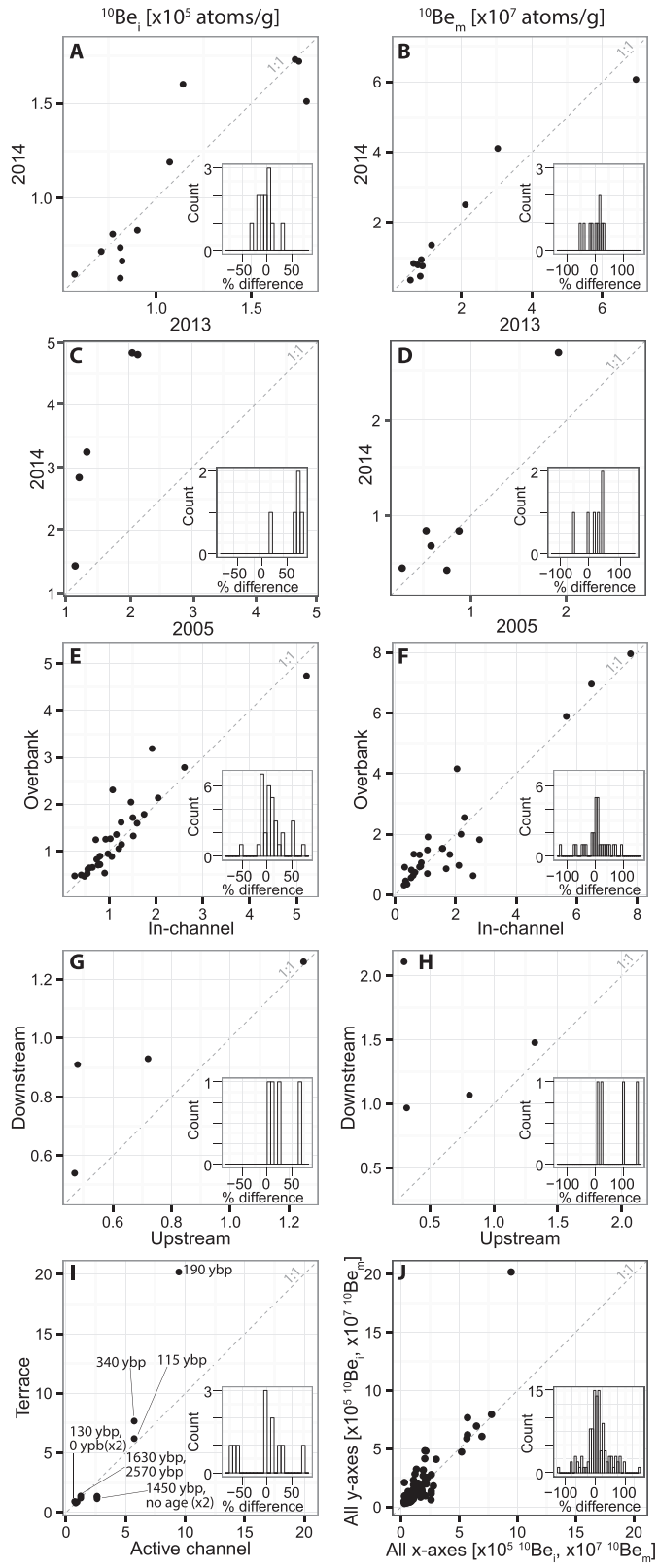

Figure 2. Temporal variation of ^{10}Be$_i$ (left column: A, C, E, G, I) and ^{10}Be$_m$ (right column: B, D, F, H) concentration for resamples (A, B) taken 6 months apart, (C, D) taken 9 years apart, (E, F) taken in-channel and overbank at the same site, (G, H) taken within 2 km of one another on the same day, and (I) terrace sands paired with active channel sediment (^{14}C ages labeled). (J) Summary plot showing all the data on plots A–I. Insets show the distribution of percentage differences between samples for each isotope and each resample period. On all histograms the bar width is 7%, which is approximately the 1σ dispersion of CRONUS N standards and 2σ dispersion for STA1(KFA) standards measured with our samples. Error bars are left off scatter plots for clarity. Data in this figure are in Supporting Information Table DR4.

tectonically active areas with high rates of human disturbance. Combining the three previously published replicate pairs (Reusser and Bierman, 2010) with our 49 pairs (Figure 5B), we find that the mode percentage difference between samples is slightly above the 2σ (7%) range for ^{10}Be$_m$.

Discussion

Overall, 43% ^{10}Be$_i$ and only 21% ^{10}Be$_m$ samples replicate within the variability of laboratory internal standards, reflecting sample preparation and analysis. However, some samples

Table III. Summary findings of temporal comparisons of isotopic concentrations. This is a summary of data shown in Supporting Information Table DR4

Temporal comparison	Isotope	Count	Samples within 1σ (6.4% for $^{10}Be_i$, 3.5% for $^{10}Be_m$)	Samples within 2σ (13% for $^{10}Be_i$, 7% for $^{10}Be_m$)	Wilcoxon test results[a] p-value	Range of % diff.	Mean % diff.	SD of % diff.
	$^{10}Be_i$	12	5	8	0.52	−33 to 34	−3	17
6 months	$^{10}Be_m$	10	0	1	0.77	−54 to 31	−2	28
	$^{10}Be_i$	5	0	0	0.06	23 to 84	69	26
Decadal	$^{10}Be_m$	6	0	1	0.44	−54 to 46	14	38
In-channel	$^{10}Be_i$	32	7	16	0.06	−52 to 72	9	25
vs. overbank	$^{10}Be_m$	29	3	7	0.29	−122 to 97	5	45
Spatial	$^{10}Be_i$	4	1	2	0.34	0.8 to 63	26	27
resamples	$^{10}Be_m$	4	0	0	0.11	12 to 150	73	65
Millennia	$^{10}Be_i$	11	3	5	0.30	−77 to 72	−6	45
	$^{10}Be_i$	64	16	32	0.76	−77 to 72	11	34
	$^{10}Be_m$	49	3	9	0.53	−122 to 150	10	46
All samples	Both	113	19	42	0.49	−122 to 150	10	39

[a]The p-value of a paired Wilcoxon test on the two populations of samples for each isotope at each time period is the probability that the two populations of samples are the same. The null hypothesis is that they are identical populations and the alternate hypothesis is two-sided.

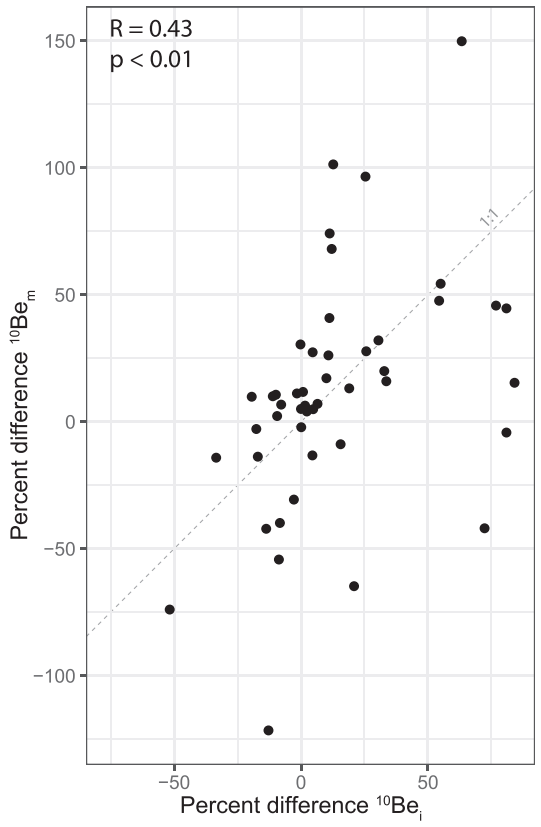

Figure 3. Correlation between percentage difference $^{10}Be_m$ and percentage difference $^{10}Be_i$ for all pairs of samples where both isotopes were measured.

replicate poorly, and in those cases individual detrital samples do not accurately characterize the behavior of the upstream watershed. For example, we find that for all replicates (considering both our new China data and previously published replicates except for Greenlandic data), individual pairs replicate within −100% to +135% difference for $^{10}Be_i$ (mean = 13.4%, standard deviation = 41%) and −122% to +150% difference for $^{10}Be_m$ (mean = 8.9%, standard deviation = 45%). Furthermore, a Mann–Whitney U-test on the absolute values of the differences (with the null hypothesis of identical populations and alternative hypothesis that $^{10}Be_i$ replicability has a greater median than $^{10}Be_m$ replicability, in other words, replicates worse), $p < 0.01$, suggesting a statistically significantly better replicability for $^{10}Be_i$ (because the p-value is so low, the null and alternate hypotheses are rejected).

Below, we explore why $^{10}Be_i$ and $^{10}Be_m$ replicate differently, consider the long-term variability in $^{10}Be_i$ concentration in river sediment, evaluate parameters and infer processes that may affect replicability, and make suggestions about sampling strategies to improve replicability in detrital samples collected not only for analysis of cosmogenic nuclides but also for other chemical and isotopic systems.

Why $^{10}Be_i$ replicates better than $^{10}Be_m$, and implications for other fallout radionuclides

The correlation between percentage difference of $^{10}Be_i$ and $^{10}Be_m$ ($R = 0.43$, $p < 0.01$) in the Chinese samples for which both isotope systems were measured indicates sediment sourcing processes in the upstream watershed are in part responsible for sample replicability over time (Figure 3). For example, if a landslide delivered a large amount of deeply sourced (and thus low isotopic concentration) material to the river between sampling times, this would affect replicability of both *in situ* and meteoric ^{10}Be, as both systems are measures of near-surface residence time (Jungers *et al.*, 2009; Graly *et al.*, 2010; Wittmann *et al.*, 2015), with the caveat that there may be differences in integration time due to varying depths of the weathering front in different places. However, 57% of the variation in replicability of $^{10}Be_m$ pairs is unexplained by $^{10}Be_i$ data. Thus processes specific to $^{10}Be_m$ must explain the remainder of the variation.

Because no landscape scale parameter we consider except upstream area significantly correlates with replicability of $^{10}Be_m$ samples such that larger basins replicate worse, in-channel sediment behavior likely explains the greater variability of $^{10}Be_m$ over time and space. In this context, it is important to note that $^{10}Be_m$ is incorporated into grain coatings of samples and that $^{10}Be_m$ concentration is controlled by grain coating thickness and composition; thus, any changes in grain coatings (such as grain disaggregation and abrasion during transport) will have a significant influence on measured $^{10}Be_m$ concentration (Singleton *et al.*, 2017) but not on $^{10}Be_i$. This influence will

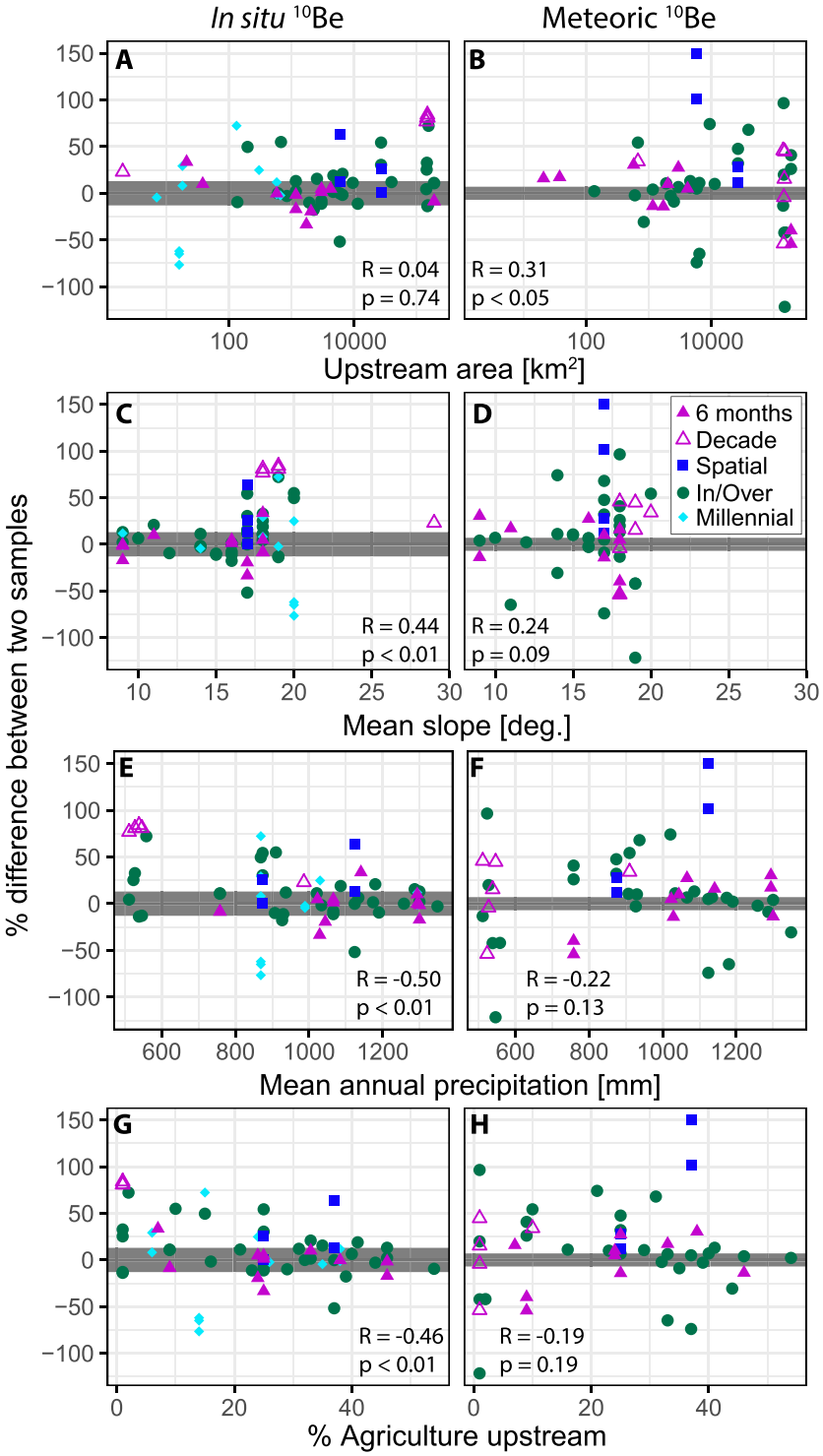

Figure 4. Percentage difference in $^{10}Be_i$ (left column: A, C, E, G) and $^{10}Be_m$ (right column: B, D, F, H) as a function of upstream area (A, B), mean basin slope (C, D), mean annual basin precipitation (E, F), and percent of the upstream watershed that is agricultural (G, H). The grey shaded area shows the range from -2σ to 2σ difference (−13% to 13% for $^{10}Be_i$, −7% to 7% for $^{10}Be_m$). Information (*R*, *p*-value) for regressions of the absolute value of the difference between samples against each parameter is shown for each plot for all data shown on each plot considered together. Note that positive *R*-values mean that there is poorer replicability for increased values of the basin average parameter, while negative *R*-values mean there is better replicability for increased values of the basin average parameter. Data shown are only the new China data. [Colour figure can be viewed at wileyonlinelibrary.com]

increase for larger basins, as we observe with the significant correlation between upstream area and replicability of $^{10}Be_m$. In contrast, $^{10}Be_i$ is measured in quartz after grain coatings have been removed. If quartz grains break down in transport, the $^{10}Be_i$ concentration will not change. Specifically, the non-conservative behavior of $^{10}Be_m$ in river systems likely explains the reason that factors that affect replicability of $^{10}Be_i$ do not also affect replicability of $^{10}Be_m$.

Another issue with $^{10}Be_m$ that does not arise with $^{10}Be_i$ is the grain size dependency of concentration (Brown *et al.*, 1988; Wittmann *et al.*, 2012; Singleton *et al.*, 2017). A prior study (Singleton *et al.*, 2017) reporting grain size data for some of our samples finds that the 250–500 μm fraction has a concentration from 0.44 to 2.02 times the concentration of the 500–850 μm fraction; the 250–500 μm and 500–850 μm fractions have 0.76–1.94 times the concentration of the

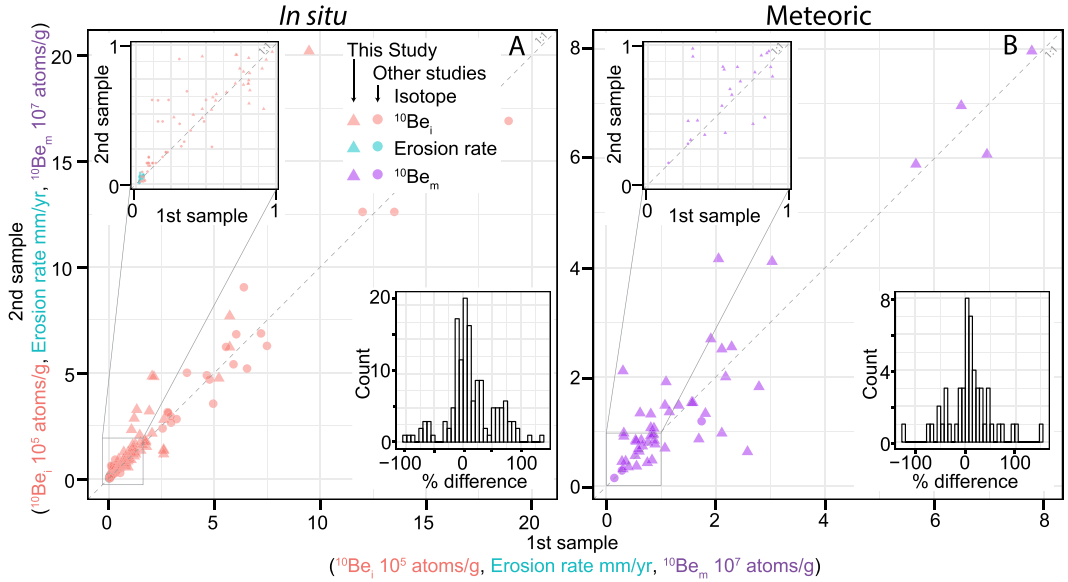

Figure 5. Summary of previously published ^{10}Be temporal replicates (circles) and our data (squares) for $^{10}Be_i$ (A, left) and $^{10}Be_m$ (B, right). Inset in the upper left is zoomed in on the lower left part of the figure. Inset in the lower right shows the distribution of the data (bin width = 7%). Data included in this figure are in Supporting Information Tables DR4, DR6 and DR7. Data plotted are from this study for Yunnan, China (n = 64, $^{10}Be_i$; and n = 49, $^{10}Be_m$), Schaller *et al.* (2002) (n = 11, erosion rates (on the $^{10}Be_i$ plot)) and Schaller et al. (2016) for Europe (n = 11, erosion rates (on the $^{10}Be_i$ plot)), Matmon *et al.* (2003) for the Great Smoky Mountains (n = 1, $^{10}Be_i$), Cox *et al.* (2009) for Madagascar (n = 2, $^{10}Be_i$), Reusser and Bierman (2010) for New Zealand (n = 3, $^{10}Be_m$), Lupker *et al.* (2012) for Nepal and India (n = 8, $^{10}Be_i$), Sosa Gonzalez *et al.* (2016) for Panama (n = 2, $^{10}Be_i$), Foster and Anderson (2016) for Colorado (n = 13, $^{10}Be_i$), Kober *et al.* (2012) for the Swiss Alps following debris flow events (n = 9, $^{10}Be_i$), Godard *et al.* (2010) for Sichuan, China (n = 2, $^{10}Be_i$), West *et al.* (2014) for Sichuan, China (n = 9, $^{10}Be_i$), Portenga *et al.* (2015) for Bhutan (n = 1, $^{10}Be_i$), Palumbo *et al.* (2011) for Tibet (n = 1, $^{10}Be_i$), Reusser *et al.* (2017) for the eastern USA (n = 1, $^{10}Be_i$), Regard *et al.* (2016) for Cameroon (n = 3), Nelson *et al.* (2014) for Greenland (n = 9), and Vance *et al.* (2003) for Nepal (n = 1, $^{10}Be_i$). $^{10}Be_i$ data are shown in red, erosion rate data in blue and $^{10}Be_m$ in purple. For Schaller *et al.* (2002, 2016) we report erosion rates because some samples are from slightly different locations and concentrations may not be consistent due to elevation differences. [Colour figure can be viewed at wileyonlinelibrary.com]

250–850 μm fraction reported in this paper (Supporting Information Table DR8). Thus, although we sieved to 250-500 μm, variations in grain size within that range could change the concentration between two time periods by as much as 100%, if one sample was only 250–500 μm sediment and the other only 500–850 μm sediment.

Stability of fallout radionuclides contained in grain coatings is dependent on the pH of the water (Boschi and Willenbring, 2016), the ability of the grain coatings to resist abrasion and the ability of the grain to withstand disaggregation (Singleton *et al.*, 2017). Although we do not have the pH of the river water taken at the same time and place as our samples, studies in the region find that the pH of local rivers, including the Mekong, Salween, Yangtze, Tsang Po and Red, is >7 and often >8 (Huang *et al.*, 2008; Shrestha *et al.*, 2008; Zhang *et al.*, 2009; Zhao *et al.*, 2013). We thus conclude that the $^{10}Be_m$ is not dissolving from the sediment grain coatings in these rivers. However, in areas where pH is more acidic, this is a potentially important concern as pH < 5 can facilitate $^{10}Be_m$ desorption (Boschi and Willenbring, 2016). Even in rivers with pH > 5, processes that physically remove the grain coatings from samples (such as abrasion during bedload movement) can alter the concentration of ^{10}Be in grain coatings. In addition, grain disaggregation can alter measured isotopic concentration. For example, in part of our study area (samples CH-114–117), prior research documents ferruginous lithic fragments that appear in thin section to be fine-grained material acting as a single coarser grain (Singleton *et al.*, 2017). The affinity of $^{10}Be_m$ for fine-grained material (Wittmann *et al.*, 2012; Laceby *et al.*, 2017; Singleton *et al.*, 2017) and the easier disaggregation of this material than minerals such as quartz or feldspar means that if these lithic fragments disaggregate during transport between two sample sites or more during one season than another, then the replicate sample will have a significantly different $^{10}Be_m$ concentration. The same issues are likely to arise for other fallout radionuclides (^{137}Cs, ^{210}Pb, ^{7}Be), which are also preferentially associated with finer-grained material, and Fe-oxide grain coatings.

Sediment storage for time periods approaching the half-life of the measured isotope can alter concentration as well. Given the small amounts of storage in most of our study area, radioactive decay or floodplain accumulation of $^{10}Be_m$ is not a concern, but with other isotopes or study areas with large floodplain systems this could be a complicating factor (Belmont *et al.*, 2014; Wittmann *et al.*, 2015). Likewise, for systems with shorter half-lives (^{137}Cs, ^{210}Pb, ^{7}Be), storage, even if over relatively short timescales, would reduce nuclide concentration.

Factors affecting replicability and process inferences

By considering correlations between reproducibility and landscape-scale characteristics such as slope and climate, we can infer processes that control sample isotope concentration over time. Processes we consider are the influence of weathering process on slopes, the transport of sediment from slopes into rivers and the downriver transport of sediment. Because changes in weathering regimes happen over longer timescales than the variability in replicability we observe, they are unlikely to be playing a role in the replicability of our samples and we do not consider weathering further.

Sediment transport processes from hillslopes to rivers likely affect both the spatial and temporal replicability of in-channel sediment samples. Movement of sediment from hillslopes to channels is not always steady but often influenced by stochastic events such as landslides and debris flows (Niemi *et al.*,

2005). Such stochastic events deliver sediment to rivers with isotopic concentrations different from material supplied by more steady creep and slopewash processes and thus can affect replicability, especially in steeper watersheds (Figure 3). This assertion is supported by our finding that mean basin upstream slope is a significant factor in replicability of $^{10}Be_i$ and explains nearly 50% of the observed variability (Figure 3). The increased variability for basins with steeper upstream slopes is expected (Binnie *et al.*, 2006; Savi *et al.*, 2014) because steeper landscapes tend to have more frequent mass wasting events, such as landslides and debris flows, which source deep material from isolated locations (Kober *et al.*, 2012). If mass wasting events happen immediately prior to sampling periods, they can significantly alter the measured isotopic concentration of sediment. However, if the events occur on timescales much longer than resampling intervals, resample analyses could replicate extremely well, but still not reflect longer-term variability in the system.

Temporal variability in contributions of sediment from different tributaries, if such tributaries have different mean elevations and thus different effective $^{10}Be_i$ production rates (Bierman *et al.*, 2005; Lupker *et al.*, 2012) or if they are eroding at different rates (Bierman *et al.*, 2005), could be responsible for the poor replicability we observe. We see evidence for varying sediment sources in the TRR resamples, which we infer to represent an increase in percentage of high-elevation, high production rate-derived sediment. Our resamples of TRR main stem Salween sites (n = 4 pairs) have $^{10}Be_i$ concentrations 77–84% higher (mean = 81%) than those originally reported by Henck *et al.* (2011); this difference is confirmed by our laboratory replicates. In these large basins (>140 000 km^2), with significant proportions (>80%) of the watersheds that drain high-elevation, low-relief parts of the Tibetan Plateau, our data are consistent with the primary sediment source changing from a deeply sourced and/or low-elevation location (e.g. if there were a large landslide in the Salween gorge) to a high-elevation location (i.e. the Tibetan Plateau) between the time that Henck *et al.* sampled in 2005 and when we sampled in 2014.

It is not possible to distinguish the effects on reproducibility of changing sediment sources over time (Lupker *et al.*, 2012) and the effects of stochastic, random sediment transport processes on hillslopes and in rivers (e.g. Cox *et al.*, 2009; Kober *et al.*, 2012). However, it is likely that smaller basins are more affected by stochastic processes (Niemi *et al.*, 2005; Yanites *et al.*, 2009), while larger basins are more affected by changes in contributions from tributaries or parts of the basin (Lupker *et al.*, 2012). Regardless of which of these two processes is driving the differences we observe, both ultimately are an issue of sediment being delivered to the channel that is not representative of the entire upstream watershed and instead is representative of just part of the watershed (Bierman *et al.*, 2005).

The effects of storage are likely minimal in the Chinese study area, given the steep topography, but could be significant in other areas. In cases where storage is significant, incision and reworking of older alluvial terraces during floods could introduce sediment with different isotope concentrations. In our study area, with limited terrace storage, the amount of sediment eroded from terraces must be small in comparison to the mass of sediment carried downstream during floods. This contrast minimizes the effect of such reworking, except perhaps just downstream of eroded outcrops. At one sample site (CH-114; one pair of replicates for both $^{10}Be_i$ and $^{10}Be_m$), where we sampled in both 2013 and 2014, the sample was taken immediately downstream of a terrace that was eroded away entirely between the 2013 and 2014 sampling trips. In this case, the samples replicate poorly (>2σ difference), consistent with the local influence of terrace erosion.

Our data can potentially identify the effects of in-channel dredging on sample replicability. At 10 different sample sites (CH-113, CH-115, CH-117, CH-133, CH-137, CH-141, CH-149, CH-157, CH-159, CH-161; 16 pairs of replicates for $^{10}Be_i$; 14 pairs for $^{10}Be_m$), mining was occurring immediately upstream of the site, samples were taken in sand and gravel mines, or an in-channel sand/gravel mine had come into the area between two sample times. Eleven of these 16 $^{10}Be_i$ pairs, but only three of the 14 $^{10}Be_m$ pairs, replicate within 2σ. Based on these data it appears that dredging has a larger effect on $^{10}Be_m$ than $^{10}Be_i$ replicability.

Effects of climate

Erosion intensifies during the monsoon (Yang *et al.*, 2010) due to heavy precipitation, which increases suspended sediment delivery and river discharge (Henck *et al.*, 2010). We find that replicability of samples in China correlates weakly with spatial differences in mean annual rainfall such that areas with more rainfall replicate better (Figure 4). However, as discussed above, we infer that this is due to a negative correlation between rainfall and slope (Supporting Information Figure DR3), rather than caused by the rainfall directly.

Paired in-channel and overbank samples allow us to test for differences in monsoon-driven seasonal sediment sourcing. Eight of 29 and 20 of 32 in-channel/over bank pairs for $^{10}Be_m$ and $^{10}Be_i$, respectively, are within 2σ of each other. However, 11 of the 32 $^{10}Be_i$ and 14 of the 29 $^{10}Be_m$ samples have statistically higher isotopic concentrations in the overbank sediment (percentage difference $> 2\sigma$), while only four out of 32 $^{10}Be_i$ and seven out of 29 $^{10}Be_m$ pairs have statistically higher isotopic concentration in the in-channel sediment (percentage difference $< -2\sigma$), suggesting that there may be a slight difference in sediment sourcing during the monsoon. A paired, one-sided Wilcoxon rank sum test (alternate hypothesis that the in-channel sample has higher concentration than the overbank sample) confirms this observation for $^{10}Be_i$ ($p < 0.05$), but not for $^{10}Be_m$ ($p = 0.15$). Although the two isotopes appear to behave differently, we argue this is due to the lower stability of $^{10}Be_m$ in the river system (see the first section of the discussion), rather than different behavior between the isotopes during the monsoon season, as both isotopes measure near-surface residence time in soils (Jungers *et al.*, 2009; Wittmann *et al.*, 2015).

Increases in ^{10}Be concentration during the monsoon season could be due to runoff sourcing more surface material via sheetwash. One possible reason for increased contributions of surface material during the monsoon season could be the common practice we observed in China of planting crops with furrows parallel to the slope rather than contour plowing. This plowing geometry appears to facilitate drainage during the rainy season. Such planting practices likely facilitate surface erosion and downslope sediment transport, thus increasing the concentration of ^{10}Be in monsoon-derived sediment. Over centuries to millennia, this would lead to a decrease in $^{10}Be_i$ concentration on slopes and an apparent increase in erosion rates for agricultural areas compared to non-agricultural areas (Von Blanckenburg *et al.*, 2004). Prior research suggests that this is the case in the more heavily agricultural parts of our study region (Schmidt *et al.*, 2016).

Another possibility is that sediment transported during the monsoon is sourced from different parts of the landscape than during the dry season. For example, monsoon season sediment could be sourced on average from higher-elevation, steeper parts of the landscape, which have higher nuclide production

rates and thus accumulate more $^{10}Be_i$ at the same erosion rate (Lupker *et al.*, 2012). These locations may not have higher accumulation rates of $^{10}Be_m$, as $^{10}Be_m$ deposition rates are correlated with mean annual precipitation (Graly *et al.*, 2011). Seasonal changes in the altitude from which sediment is derived would provide an explanation for the statistically significant difference in $^{10}Be_i$ but not $^{10}Be_m$ in in-channel and overbank sediments.

Long-timescale changes in $^{10}Be_i$

Although the population of in-channel samples does not have a statistically different concentration of $^{10}Be_i$ when compared with the population of buried terrace sand samples in China, and the mode of the population of differences is around 0%, only five of 11 pairs replicate within 13%. Of the six pairs that do not replicate within 13%, they are evenly split between samples with higher concentrations in terrace sands and higher concentrations in active channel sediments. Furthermore, the two samples with the lowest difference in concentration between terrace and active channel sediments are the youngest and oldest terrace samples (CH-040, 0 ± 20 ^{14}C ybp, −2.3% different; CH-124, 2570 ± 20 ^{14}C ybp, −1.2% different). In addition, there is no relationship between percentage difference in concentration and the age of the terrace.

Measurement of $^{10}Be_i$ in terrace and adjacent stream channel sediment indicates there has not been a systematic change in isotopic concentration and thus sediment sourcing or erosion rates across the region over the last 2500 ^{14}C years (Figure 2 and Table III). The lack of systematic variation over time between buried terrace and active channel samples suggests that overall human activity has not substantially changed cosmogenically based estimates of long-term erosion rates, although there may be effects in specific, heavily impacted basins.

In our study area, human activity dates back to at least 5000 ^{14}C years before present (Liu *et al.*, 2016), suggesting that there were people living in the areas we sampled prior to the time the oldest terraces we sampled formed. However, the degree to which individuals in these settlements were engaged in agriculture is currently debated (d'Alpoim Guedes, 2015, 2016). Thus it is possible that the $^{10}Be_i$ concentrations in terrace sediments were affected by early human activities in China. We think this unlikely because the terraces we sampled are in relatively small watersheds (<700 km^2) without known archaeological sites and because early human impacts, prior to mechanization, were far less intensive than those occasioned in the last half a century.

Previously published data from Europe and Madagascar also compare terrace sediment to active channel sediment to elucidate longer-term variability in $^{10}Be_i$ concentration and derived erosion rates. In Madagascar, terraces at least 1000 years old have isotopic concentrations between 9% less and 30% more than active channel sediment (Cox *et al.*, 2009). The sample which replicates well is from a basin with few *lavakas* (deep erosional gullies), while the one which replicates poorly (>13% different, using our 2σ metric) is from a basin with many *lavakas*, suggesting that poor replication results from deep erosional features driving long-term variability in isotope concentration. In Europe, samples of sediment from terraces and active channels vary considerably (−100% to 91% difference) for deposits ranging from 1350 years old to 2 million years old (Schaller *et al.*, 2002, 2016). The age of the terrace does not correlate with difference between modern sediment- and terrace sediment-derived erosion rates. Here, the authors infer that erosion rates shift as a result of changing climate (Schaller *et al.*, 2002, 2016) over glacial/interglacial timescales.

Sampling strategies to improve representativeness of detrital samples

Our new data and a compilation of existing replication data suggest caution in the interpretation of single detrital sediment samples in areas with many deep erosional features (such as steep, tectonically active landscapes) or widespread agricultural land use. In less disturbed landscapes, even after large storms individual samples appear to remain representative of the upstream watershed.

By using internal standards in our analysis, we document that analytically introduced variance (2σ level) is 7–13% depending on the ^{10}Be isotopic system; yet we find as much as 150% difference in the isotopic concentration of paired resamples, suggesting that the bulk of the difference we and others measure is coming from geological processes operating on slopes and in channels and not from sample processing. Knowing that much of the variance is geological suggests means to overcome it.

For $^{10}Be_i$, large populations of samples and their corresponding resamples have similar modes and means – these large datasets are effectively averaging over time and space. Field sampling techniques can mimic such averaging. For example, one could amalgamate multiple samples separated in time or slightly in space (e.g. in-channel and overbank sediments) in order to represent better the isotopic character of the upstream area; this approach has been used before to improve the accuracy of erosion rate and sediment transport estimates (e.g. Nichols *et al.*, 2005; Carretier *et al.*, 2013).

Much poorer reproducibility in the $^{10}Be_m$ system (likely due to the isotope's incorporation in potentially unstable grain coatings rather than mineral lattices) may confound sampling strategies. If $^{10}Be_m$ is to be used in a way that requires the assumption of well-mixed samples and representative sourcing from upstream areas (Reusser and Bierman, 2010; Willenbring and von Blanckenburg, 2010; Wittmann *et al.*, 2015; Rahaman *et al.*, 2017), the sampling strategies we propose for $^{10}Be_i$ should reduce the variability inherent in this system, but will not account for changes in grain coatings caused by dissolution and/or abrasion during transport.

The impact on experimental results of temporal and spatial variability in isotope concentration depends on the nature of the study area. In study areas with high variability in isotopic concentration across catchments (such as our Chinese field area where measured concentrations of ^{10}Be vary by nearly two orders of magnitude), the effects of poor spatial or temporal replicability (up to a factor of ~2) will be minimal compared to overall differences in isotopic concentration correlated with geological and environmental metrics such as topography, mean annual precipitation and lithology. An amalgamated sampling scheme, such as we recommend, will further reduce the effects of temporally variable ^{10}Be concentrations in fluvial sediment. However, in study areas where erosion rates vary little between watersheds but disturbance levels are high, even amalgamating samples may not remove the effects of poor replicability on study data. Likewise, if there are low-frequency, high-magnitude events that occur on timescales longer than the sampling frequency or the depositional duration of terrace sediment, then even an amalgamated sampling strategy will fail to reflect geological processes that could contribute to changing isotopic concentration in sediment in the watershed.

Conclusions

This, the first compilation and analysis of replication data for both meteoric and *in situ* cosmogenic ^{10}Be measured in fluvial sediment, finds that while central tendencies are similar, many replicates show scatter beyond that expected analytically. For example, of the 148 replicate samples analyzed so far for $^{10}Be_i$ and the 52 for $^{10}Be_m$, 124 individual pairs of samples replicate poorly ($>2\sigma$ difference) relative to the analytical replicability of internal standards, whereas 76 pairs replicate within 2σ. Reproducibility for $^{10}Be_i$ is much better than for $^{10}Be_m$, calling into question the meaning of single sample measurements of $^{10}Be_m$ and perhaps explaining the scatter in results from this system (Wittmann *et al.,* 2015).

We find that environments with widespread agriculture, long-term climate change, steep slopes or deep erosional features are likely to have temporal replicate samples that agree poorly. In such environments, we recommend an amalgamated sampling scheme to ensure that samples are more representative of long-term rates than single-point samples. Research that relies on detrital samples being well mixed and thus representative of the entire upstream area will benefit from adopting sampling strategies that mix samples taken either at different times or places to improve representativeness of such samples.

Our study suggests that paired replicate samples can be used to infer processes acting on a watershed over seasons or years. For example, variability in mean basin steepness explains nearly 50% of the observed variability in replicate samples for *in situ* ^{10}Be, suggesting that processes occurring in steep landscapes (e.g. landslides and debris flows) have a major effect on the replicability of samples. The results in this study suggest that continuing to use ^{10}Be and other detrital systems to identify variability rather than just average erosion rates is likely to improve our understanding of temporal changes in sediment sourcing and erosional processes.

Acknowledgements—Research was supported by funding from the US National Science Foundation awarded to A. H. Schmidt (NSF-EAR-1114166), P. R. Bierman (NSF-EAR-1114159) and D. H. Rood (NSF-EAR-1114436). We thank L. Corbett, A. Lubeck and J. Southon for the ^{14}C analyses of charcoal samples, and staff of the AMS laboratory at SUERC and LLNL for support during ^{10}Be isotopic analyses. The authors thank D. McPhillips for collecting and providing sample Y13-01-DM and for feedback on an early version of the manuscript. We thank T. Neilson, C. M. Zhang, R. J. Wei, J. A. Bower, A. Singleton, and Y. Qiu for field assistance. We thank T. Neilson for CH-0xx sample analyses, A. Denn for the TRR lab replicate analyses, and J. Martin for GIS analyses and for drafting the data repository figures. We thank two anonymous reviewers and an associate editor for constructive feedback that improved the manuscript.

References

d'Alpoim Guedes J. 2015. Rethinking the spread of agriculture to the Tibetan Plateau. *The Holocene* **25**: 1498–1510.

d'Alpoim Guedes J. 2016. Model building, model testing, and the spread of agriculture to the Tibetan Plateau. *Archaeological Research in Asia* **5**: 16–23.

Andermann C, Bonnet S, Gloaguen R. 2011. Evaluation of precipitation data sets along the Himalayan front. *Geochemistry, Geophysics, Geosystems* **12**: Q07023. https://doi.org/10.1029/2011GC003513.

Belmont P, Willenbring JK, Schottler SP, Marquard J, Kumarasamy K, Hemmis JM. 2014. Toward generalizable sediment fingerprinting with tracers that are conservative and nonconservative over sediment routing timescales. *Journal of Soils and Sediments* **14**: 1479–1492.

Bernet M, Spiegel C. 2004. *Detrital Thermochronology*. Geological Society of America: Boulder, CO.

Bierman PR, Steig EJ. 1996. Estimating rates of denudation using cosmogenic isotope abundances in sediment. *Earth Surface Processes and Landforms* **21**: 125–139.

Bierman PR, Reuter JM, Pavich M, Gellis AC, Caffee MW, Larsen J. 2005. Using cosmogenic nuclides to contrast rates of erosion and sediment yield in a semi-arid, arroyo-dominated landscape, Rio Puerco Basin, New Mexico. *Earth Surface Processes and Landforms* **30**: 935–953.

Binnie SA, Phillips WM, Summerfield MA, Fifield LK. 2006. Sediment mixing and basin-wide cosmogenic nuclide analysis in rapidly eroding mountainous environments. *Quaternary Geochronology* **1**: 4–14.

Binnie SA, Phillips WM, Summerfield MA, Fifield LK. 2007. Tectonic uplift, threshold hillslopes, and denudation rates in a developing mountain range. *Geology* **35**: 743–746.

von Blanckenburg F, Bouchez J, Wittmann H. 2012. Earth surface erosion and weathering from the Be-10 (meteoric)/Be-9 ratio. *Earth and Planetary Science Letters* **351**: 295–305.

Boschi V, Willenbring JK. 2016. Beryllium desorption from minerals and organic ligands over time. *Chemical Geology* **439**: 52–58.

Brown L, Pavich MJ, Hickman RE, Klein J, Middleton R. 1988. Erosion of the Eastern United States observed with ^{10}Be. *Earth Surface Processes and Landforms* **13**: 441–457.

Brown ET, Stallard RF, Larsen MC, Raisbeck GM, Yiou F. 1995. Denudation rates determined from the accumulation of in-situ produced ^{10}Be in the Luquillo Experimental Forest, Puerto Rico. *Earth and Planetary Science Letters* **129**: 193–202.

Buck S. 2015. Solving reproducibility. *Science* **348**: 1403–1403.

Carretier S, Regard V, Vassallo R, Aguilar G, Martinod J, Riquelme R, Pepin E, Charrier R, Hérail G, Farías M. 2013. Slope and climate variability control of erosion in the Andes of central Chile. *Geology* **41**: 195–198.

Chen J, Chen J, Liao A, Cao X, Chen L, He C, Han G, Peng S, Lu M, Zhang W, Tong X, Mills J. 2015. Global land cover mapping at 30 m resolution: a POK-based operational approach. *ISPRS Journal of Photogrammetry and Remote Sensing* **103**: 7–27.

Clapp E, Bierman PR, Caffee M. 2002. Using ^{10}Be and ^{26}Al to determine sediment generation rates and identify sediment source areas in an arid region drainage basin. *Geomorphology* **45**: 89–104.

Corbett LB, Bierman PR, Rood DH. 2016. An approach for optimizing *in situ* cosmogenic ^{10}Be sample preparation. *Quaternary Geology* **33**: 24–34.

Cox R, Bierman PR, Jungers MC, Rakotondrazafy AFM. 2009. Erosion rates and sediment sources in Madagascar inferred from ^{10}Be analysis of lavaka, slope, and river sediment. *Journal of Geology* **117**: 363–376.

Editorial Staff. 2016a. Go forth and replicate. *Nature* **536**: 373.

Editorial Staff. 2016b. Let's think about cognitive bias. *Nature* **526**: 163.

Editorial Staff. 2016c. Repetitive flaws. *Nature* **529**: 256.

Editorial Staff. 2017. Promoting reproducibility with registered reports. *Nature Human Behavior*: 1. https://doi.org/10.1038/s41562-016-0034.

Foster MA, Anderson RS. 2016. Assessing the effect of a major storm on ^{10}Be concentrations and inferred basin-averaged denudation rates. *Quaternary Geochronology*. https://doi.org/10.1016/j.quageo.2016.03.006.

Godard V, Lave J, Carcaillet J, Cattin R, Bourles D, Zhu J. 2010. Spatial distribution of denudation in Eastern Tibet and regressive erosion of plateau margins. *Tectonophysics* **491**: 253–274.

Goldstein S, Hofmann A, Lehnert K, Andreae M, Arndt N, Baker J, Barth A, Bendall C, Bourdon B, Carlson R. 2014. Requirements for the publication of geochemical data. *Integrated Earth Data Applications*: 96. https://doi.org/10.1029/2015EO022207.

Goodman SN, Fanelli D, Ioannidis JPA. 2016. What does research reproducibility mean? *Science Translational Medicine* **8** 341ps12, doi:https://doi.org/10.1126/scitranslmed.aaf5027.

Graly JA, Bierman PR, Reusser LJ, Pavich MJ. 2010. Meteoric ^{10}Be in soil profiles: a global meta-analysis. *Geochimica et Cosmochimica Acta* **74**: 6814–6829.

Graly JA, Reusser LJ, Bierman PR. 2011. Short and long-term delivery rates of meteoric ^{10}Be to terrestrial soils. *Earth and Planetary Science Letters* **302**: 329–336.

Gran KB, Czuba JA. 2017. Sediment pulse evolution and the role of network structure. *Geomorphology* **277**: 17–30.

Granger DE, Kirchner JW, Finkel RC. 1996. Spatially averaged long-term erosion rates measured from in-situ produced cosmogenic nuclides in alluvial sediment. *Journal of Geology* **104**: 249–257.

Hanson B, Hilst R. 2014. AGU's data policy: history and context. *Eos, Transactions American Geophysical Union* **95**: 337.

Harel M-A, Mudd S, Attal M. 2016. Global analysis of the stream power law parameters based on worldwide ^{10}Be denudation rates. *Geomorphology* **268**: 184–196.

Henck AC, Montgomery DR, Huntington KW, Liang C. 2010. Monsoon control of effective discharge, Yunnan and Tibet. *Geology* **38**: 975–978.

Henck AC, Huntington KW, Stone JO, Montgomery DR, Hallet B. 2011. Spatial controls on erosion in the Three Rivers Region, southeastern Tibet and southwestern China. *Earth and Planetary Science Letters* **303**: 71–83.

Herman F, Beyssac O, Brughelli M, Lane SN, Leprince S, Adatte T et al. 2015. Erosion by an Alpine glacier. *Science* **350**: 193–195.

Hewawasam T, Von Blanckenburg F, Schaller M, Kubik PW. 2003. Increase of human over natural erosion rates in tropical highlands constrained by cosmogenic nuclides. *Geology* **33**: 597–600.

Huang X, Sillanpää M, Duo B, Gjessing ET. 2008. Water quality in the Tibetan Plateau: metal contents of four selected rivers. *Environmental Pollution* **156**: 270–277.

Jull AJT, Scott EM, Bierman P. 2015. The CRONUS-Earth inter-comparison for cosmogenic isotope analysis. *Quaternary Geochronology* **26**: 3–10.

Jungers MC, Bierman PR, Matmon A, Nichols K, Larsen J, Finkel R. 2009. Tracing hillslope sediment production and transport with in situ and meteoric^{10}Be. *Journal of Geophysical Research* **114**. https://doi.org/10.1029/2008jf001086.

Kober F, Hippe K, Salcher B, Ivy-Ochs S, Kubik PW, Wacker L, Hahlen N. 2012. Debris-flow-dependent variation of cosmogenically derived catchment-wide denudation rates. *Geology* **40**: 935–938.

Kohl CP, Nishiizumi K. 1992. Chemical isolation of quartz for measurement of in-situ produced cosmogenic nuclides. *Geochimica et Cosmochimica Acta* **56**: 3583–3587.

Laceby JP, Evrard O, Smith HG, Blake WH, Olley JM, Minella JPG, Owens PN. 2017. The challenges and opportunities of addressing particle size effects in sediment source fingerprinting: a review. *Earth-Science Reviews*. https://doi.org/10.1016/j.earscirev.2017.04.009.

Lal D. 1991. Cosmic ray labeling of erosion surfaces: *in situ* nuclide production rates and erosion models. *Earth and Planetary Science Letters* **104**: 424–439.

Lal D, Peters B. 1967. *Cosmic Ray Produced Radioactivity on the Earth*. Springer: Berlin; 551–612.

Liu H, Cui Y, Zuo X, Li H, Wang J, Zhang D, Zhang J, Dong G. 2016. Human settlements and plant utilization since the late prehistoric period in the Nujiang River valley, Southeast Tibetan Plateau. *Archaeological Research in Asia* **5**: 63–71.

Lupker M, Blard PH, Lave J, France-Lanord C, Leanni L, Puchol N, Charreau J, Bourles D. 2012. Be-10-derived Himalayan denudation rates and sediment budgets in the Ganga basin. *Earth and Planetary Science Letters* **333**: 146–156.

Matmon A, Bierman PR, Larsen J, Southworth S, Pavich MJ, Finkel RC, Caffee MW. 2003. Erosion of an ancient mountain range, the Great Smoky Mountains, North Carolina and Tennessee. *American Journal of Science* **303**: 517–855.

McNutt M. 2014. Reproducibility. *Science* **343**: 229–229.

McPhillips D, Brandon MT. 2010. Using tracer thermochronology to measure modern relief change in the Sierra Nevada, California. *Earth and Planetary Science Letters* **296**: 373–383.

McPhillips D, Bierman PR, Rood DH. 2014. Millennial-scale record of landslides in the Andes consistent with earthquake trigger. *Nature Geoscience* **7**: 925–930.

Miller DJ, Benda LE. 2000. Effects of punctuated sediment supply on valley-floor landforms and sediment transport. *Geological Society of America Bulletin* **112**: 1814–1824.

Montgomery DR, Brandon MT. 2002. Topographic controls on erosion rates in tectonically active mountain ranges. *Earth and Planetary Science Letters* **201**: 481–489.

NASA LP-DAAC. 2012. *ASTER GDEM*. NASA Land Processes Distributed Active Archive Center: Sioux Falls, SD.

Neilson TB. 2015. Using long- and short-lived sediment-associated isotopes to track erosion and sediment movement through rivers in Yunnan, SW China. Master of Science thesis, University of Vermont, Burlington, VT.

Nelson AH, Bierman PR, Shakun JD, Rood DH. 2014. Using in situ cosmogenic ^{10}Be to identify the source of sediment leaving Greenland. *Earth Surface Processes and Landforms* **39**: 1087–1100.

Nichols KK, Bierman PR, Caffee M, Finkel R, Larsen J. 2005. Cosmogenically enabled sediment budgeting. *Geology* **33**: 133–136.

Niemi NA, Oskin M, Burbank DW, Heimsath AM, Gabet EJ. 2005. Effects of bedrock landslides on cosmogenically determined erosion rates. *Earth and Planetary Science Letters* **237**: 480–498.

NIH. 2016a. *Policy and Compliance: Rigor and Reproducibility*. National Institutes of Health Grants and Funding. Available: https://grants.nih.gov/reproducibility/index.htm [22 February 2017].

NIH. 2016b. *Research and Training: Rigor and Reproducibility*. National Institutes of Health. Available: https://www.nih.gov/research-training/rigor-reproducibility [22 February 2017].

Nishiizumi K, Imamura M, Caffee MW, Southon JR, Finkel RC, McAninch J. 2007. Absolute calibration of ^{10}Be AMS standards. *Nuclear Instruments and Methods B* **258**: 403–413.

NSF. 2014. *A framework for ongoing and future National Science Foundation activities to improve reproducibility, replicability, and robustness in funded research*. Office of Management and Budget: Washington, DC.

NSF. 2016. Dear colleague letter: encouraging reproducibility in computing and communications research. National Science Foundation: Arlington, VA.

Owens PN, Blake WH, Gaspar L, Gateuille D, Koiter AJ, Lobb DA, Petticrew EL, Reiffarth DG, Smith HG, Woodward JC. 2016. Fingerprinting and tracing the sources of soils and sediments: Earth and ocean science, geoarchaeological, forensic, and human health applications. *Earth-Science Reviews* **162**: 1–23.

Palumbo L, Hetzel R, Tao M, Li X. 2011. Catchment-wide denudation rates at the margin of NE Tibet from in situ-produced cosmogenic ^{10}Be. *Terra Nova* **23**: 42–48.

Portenga EW, Bierman PR. 2011. Understanding Earth's eroding surface with ^{10}Be. *GSA Today* **21**: 4–10.

Portenga EW, Bierman PR, Duncan C, Corbett LB, Kehrwald NM, Rood DH. 2015. Erosion rate of the Bhutanese Himalaya determined using *in situ*-produced ^{10}Be. *Geomorphology* **233**: 112–126.

Rahaman W, Wittmann H, von Blanckenburg F. 2017. Denudation rates and the degree of chemical weathering in the Ganga River basin from ratios of meteoric cosmogenic ^{10}Be to stable ^{9}Be. *Earth and Planetary Science Letters* **469**: 156–169.

Regard V, Carretier S, Boeglin J-L, Ndam Ngoupayou J-R, Dzana J-G, Bedimo Bedimo J-P, Riotte J, Braun J-J. 2016. Denudation rates on cratonic landscapes: comparison between suspended and dissolved fluxes, and ^{10}Be analysis in the Nyong and Sanaga River basins, south Cameroon. *Earth Surface Processes and Landforms* **41**: 1671–1683.

Reusser LJ, Bierman PR. 2010. Using meteoric ^{10}Be to track fluvial sand through the Waipaoa River basin, New Zealand. *Geology* **38**: 47–50.

Reusser LJ, Bierman PR, Rizzo DM, Portenga EW, Rood DH. 2017. Characterizing landscape-scale erosion using ^{10}Be in detrital fluvial sediment: slope-based sampling strategy detects the effect of widespread dams. *Water Resources Research* **53**: 4476–4486.

Rosenblatt M. 2016. An incentive-based approach for improving data reproducibility. *Science Translational Medicine* **8**: 336ed5. https://doi.org/10.1126/scitranslmed.aaf5003.

Ruhl K, Hodges K. 2005. The use of detrital mineral cooling ages to evaluate steady state assumptions in active orogens: an example from the central Nepalese Himalaya. *Tectonics* **24**. https://doi.org/10.1029/2004TC001712.

Santos GM, Moore RB, Southon JR, Griffin S, Hinger E, Zhang D. 2007. AMS ^{14}C sample preparation at the KCCAMS/UCI facility: status report and performance of small samples. *Radiocarbon* **49**: 255–269.

Savi S, Norton K, Picotti V, Brardinoni F, Akçar N, Kubik PW, Delunel R, Schlunegger F. 2014. Effects of sediment mixing on ^{10}Be concentrations in the Zielbach catchment, central-eastern Italian Alps. *Quaternary Geochronology* **19**: 148–162.

Schaller M, von Blanckenburg F, Veldkamp A, Tebbens LA, Hovius N, Kubik PW. 2002. A 30 000 yr record of erosion rates from cosmogenic ^{10}Be in Middle European river terraces. *Earth and Planetary Science Letters* **204**: 307–320.

Schaller M, Ehlers T, Stor T, Torrent J, Lobato L, Christl M, Vockenhuber C. 2016. Spatial and temporal variations in denudation rates derived from cosmogenic nuclides in four European fluvial terrace sequences. *Geomorphology* **274**: 180–192.

Schmidt AH, Neilson TB, Bierman PR, Rood DH, Ouimet WB, Sosa GV. 2016. Influence of topography and human activity on apparent in situ ^{10}Be-derived erosion rates in Yunnan, SW China. *Earth Surface Dynamics* **4**: 819–830.

Shrestha S, Kazama F, Nakamura T. 2008. Use of principal component analysis, factor analysis and discriminant analysis to evaluate spatial and temporal variations in water quality of the Mekong River. *Journal of Hydroinformatics* **10**: 43–56.

Singleton AA, Schmidt AH, Bierman PR, Rood DH, Neilson TB, Greene ES, Bower JA, Perdrial N. 2017. Effects of grain size, mineralogy, and acid-extractable grain coatings on the distribution of the fallout radionuclides ^{7}Be, ^{10}Be, ^{137}Cs, and ^{210}Pb in river sediment. *Geochimica et Cosmochimica Acta* **197**: 71–86.

Sosa Gonzalez V. 2016. Erosion rates in subtropical, rapidly developing countries: an isotopic approach to measuring background rates of erosion in Brazil and China. PhD thesis, Rubenstein School of Natural Resources, University of Vermont, Burlington, VT.

Sosa Gonzalez V, Bierman PR, Nichols KK, Rood DH. 2016. Long-term erosion rates of Panamanian drainage basins determined using in situ ^{10}Be. *Geomorphology* **268**: 54–63.

Stone J. 1998. A rapid fusion method for separation of beryllium-10 from soils and silicates. *Geochimica et Cosmochimica Acta* **62**: 555–561.

Vance D, Bickle M, Ivy-Ochs S, Kubik PW. 2003. Erosion and exhumation in the Himalaya from cosmogenic isotope inventories of river sediments. *Earth and Planetary Science Letters* **206**: 273–288.

Vermeesch P. 2007. Quantitative geomorphology of the White Mountains (California) using detrital apatite fission track thermochronology. *Journal of Geophysical Research - Earth Surface* **112**. https://doi.org/10.1029/2006JF000671.

Von Blanckenburg F, Hewawasam T, Kubik PW. 2004. Cosmogenic nuclide evidence for low weathering and denudation in the wet, tropical highlands of Sri Lanka. *Journal of Geophysical Research - Earth Surface* **109**. https://doi.org/10.1029/2003JF000049.

Wainer H. 2012. The survival of the fittists. *American Scientist* **100**: 358–361.

West AJ, Hetzel R, Li G, Jin ZD, Zhang F, Hilton RG, Densmore AL. 2014. Dilution of Be-10 in detrital quartz by earthquake-induced landslides: implications for determining denudation rates and potential to provide insights into landslide sediment dynamics. *Earth and Planetary Science Letters* **396**: 143–153.

Willenbring JK, von Blanckenburg F. 2010. Meteoric cosmogenic Beryllium-10 adsorbed to river sediment and soil: applications for Earth-surface dynamics. *Earth-Science Reviews* **98**: 105–122.

Willenbring JK, Codilean AT, McElroy B. 2013. Earth is (mostly) flat: apportionment of the flux of continental sediment over millennial time scales. *Geology* **41**: 343–346.

Wittmann H, Von Blanckenburg F, Bouchez J, Dannhaus N, Naumann R, Christl M, Gaillardet J. 2012. The dependence of meteoric ^{10}Be concentrations on particle size in Amazon River bed sediment and the extraction of reactive ^{10}Be/^{9}Be ratios. *Chemical Geology* **318–319**: 126–138.

Wittmann H, Blanckenburg F, Dannhaus N, Bouchez J, Gaillardet J, Guyot J-L, Maurice L, Roig H, Filizola N, Christl M. 2015. A test of the cosmogenic ^{10}Be (meteoric)/^{9}Be proxy for simultaneously determining basin-wide erosion rates, denudation rates, and the degree of weathering in the Amazon basin. *Journal of Geophysical Research - Earth Surface* **120**: 2498–2528.

Xu S, Freeman SPHT, Rood DH, Shanks RP. 2015. Decadal Be-10, Al-26 and Cl-36 QA measurements on the SUERC 5 MV accelerator mass spectrometer. *Nuclear Instruments and Methods in Physics Research Section B: Beam Interactions with Materials and Atoms* **361**: 39–42.

Yang ZS, Yang LF, Zhang BS. 2010. Soil erosion and its basic characteristics at karst rocky-desertified land consolidation area: a case study at Muzhe Village of Xichou County in Southeast Yunnan, China. *Journal of Mountain Science* **7**: 55–72.

Yanites BJ, Tucker GE, Anderson RS. 2009. Numerical and analytical models of cosmogenic radionuclide dynamics in landslide-dominated drainage basins. *Journal of Geophysical Research - Earth Surface*: 114. https://doi.org/10.1029/2008JF001088.

Yatagai A, Kamiguchi K, Arakawa O, Hamada A, Yasutomi N, Kitoh A. 2012. APHRODITE: constructing a long-term daily gridded precipitation dataset for Asia based on a dense network of rain gauges. *Bulletin of the American Meteorological Society* **39**: 1401–1415.

Zhang Q, Li Z, Zeng G, Li J, Fang Y, Yuan Q, Wang Y, Ye F. 2009. Assessment of surface water quality using multivariate statistical techniques in red soil hilly region: a case study of Xiangjiang watershed, China. *Environmental Monitoring and Assessment* **152**: 123–131.

Zhang X, Huang C, Wang Y, Clift PD, Yan Y, Fu X, Chen D. 2017. Evolving Yangtze River reconstructed by detrital zircon U-Pb dating and petrographic analysis of Miocene marginal sea sedimentary rocks of the Western Foothills and Hengchun Peninsula, Taiwan. *Tectonics* **36**: 634–651.

Zhao P, Tang X, Tang J, Wang C. 2013. Assessing water quality of Three Gorges Reservoir, China, over a five-year period from 2006 to 2011. *Water Resources Management* **27**: 4545–4558.

Supporting Information

Additional Supporting Information may be found online in the supporting information tab for this article.

Figure DR1: Topographic, land use, climate, and geologic context for the study. Geology is from USGS (2008), land use from Chen et al. (2015), and topography information from HydroSHEDS. (A) Geology of the study area. (B) Elevation and sample locations. (C) Slope. (D) Mean annual rainfall. (E) Mean local relief over a move 5 km radius window. (F) Land use and land cover.

Figure DR2A: Stratigraphic column for samples CH-006 and CH-007.

Figure DR2B: Stratigraphic column for samples CH-008.

Figure DR2C: Stratigraphic column for samples CH-018 and CH-019.

Figure DR2D: Stratigraphic column for sample CH-022.

Figure DR2E: Stratigraphic column for sample CH-038.

Figure DR2F: Stratigraphic column for sample CH-040.

Figure DR2G: Stratigraphic column for sample CH-051.

Figure DR2H: Stratigraphic column for samples CH-123, CH-124, and CH-125.

Table DR1. Supporting Information

Table DR2. Supporting Information

Table DR3. Supporting Information

Table DR4. Supporting Information

Table DR5. Supporting Information

Table DR6. Supporting Information

Table DR7. Supporting Information

Table DR8. Supporting Information